

Through-Life Assessment of Ductile Tearing under Low-Constraint Conditions

V.P. Naumenko¹

¹*G.S. Pisarenko Institute for Problems of Strength, Kyiv, Ukraine*

Abstract

The paper outlines an innovative test procedure aimed at a comprehensive assessment of plane stress tearing in sheet metals and some results of its validation. This study gives an additional ground for updating the procedure by taking into account several experimental findings on the formation and extension of two slanted cracks emanating from a single open hole in plate-type specimens. The focus is on contrasting the ductile fracture behaviour under uncontained yielding in specimens with a small and a relatively large width-to-thickness ratio.

1. Introduction

Currently, the acceptance levels for crack-like flaws in damage-tolerant components are usually defined based on the concept of Fitness-For-Service (FFS). Thus, a particular component is considered to be adequate for its service requirements, provided that conditions causing failure are not reached. If cracks are detected, the rejection or repair of a component is justified using multi-level engineering approaches similar to [1]. Although the FFS procedures are employed by numerous organizations, there is no unified method for through-life assessment of tearing in sheet metals. Here, the term *through-life assessment* means that all measures of tear resistance can be determined continuously (from the nucleation of a tear crack and up to the complete separation) or in a point-by-point manner for test events of practical importance. This technique of collecting and analysing test data was developed in the framework of an engineering concept of plane stress tearing called Unified Methodology (UM) of fracture investigation [2-8]. It was recently used for assessing the Steady State Tearing (SST) in thin plates of a high-strength low-hardening aluminium alloy [8].

2. Main features of UM-based FFS procedure

The self-consistent FFS procedure based on the UM is employed for unified assessment of tearing in sheet metals exhibiting purely elastic, elastic-plastic, and purely plastic fracture behaviour. It is a single tool for evaluation of the stress-, displacement-, and energy-based measures of fracture resistance. They are estimated from the results of testing laboratory-sized specimens of the same type in uniaxial tension under quasi-fixed grip conditions. An important point is that the characteristics of plastic flow, localized damaging, and cracking all are treated

¹ 2 Timiryazievskaya str., Kyiv 01014, Ukraine, Tel. +38 044 286 6857, E-mail: v.p.naumenko@ipp.kiev.ua

as inherently dependent on the in-plane size and shape of the plate-type specimens, as well as on the outer boundary restraints.

For an FFS procedure with such a broad scope, it is appropriate to use mechanical parameters that can be quantified using a well-defined technique. Therefore, the UM focuses on changes in the geometry of the whole crack border instead of considering mainly crack-tip displacements, which are given much attention in the current fracture mechanics analysis. It deals with the spacing and displacement of the so-called extreme points m , n on the inner and M , N on the outer boundaries (see Fig. 1a) of a rectangular Problem Domain (PD). The displacements $v(m)$, $u(n)$, $v(M)$, and $u(N)$ are used to relate changes in the global geometries of the crack and the outer PD boundaries. The test data collected are presented as functions of the applied load. A schematic diagram of pop-in fracture under displacement-controlled loading is shown in Fig. 2.

Generally, ductile tearing can be seen as an interplay of four concurrent processes represented by the through-life fracture curves (Fig. 3) that characterize the step-wise cracking (*i-s-f* curve), incubation of localized damage ahead of the crack tips (*i-d-f*), attainment of the zero crack tip stresses (*i-n-f*), and formation of specific stress-strain fields in a fully unloaded specimen (*i-u-f*). These curves, except for (*i-n-f*), can be plotted using the test records P vs. $2c$ and P vs. $2v(m)$, where $2v(m)$ is the Crack Mouth Opening Displacement (CMOD). To construct the post-test fracture curve (*i-n-f*), the Crack Mouth Opening Spacing (CMOS)- $2s(m)_n$ and the corresponding crack length $2c_n$ should be measured in pairs using the upper and lower halves of the fully fractured specimen, as shown in [8]. Thus, geometric changes in the inner and outer boundaries are assessed jointly for a loaded (moving crack), fully unloaded (arrested crack), and broken-down (fully developed crack) specimen.

Assume that an undeformed, undamaged, and unstressed specimen contains a small stress raiser with the simplest geometry (Fig. 1c). Shortly after the application of the tensile load P acting across the crack growth line, two localized necks start forming inboard of the plate, namely, ahead of the points n , as it was observed in [9]. Plastic deformation and damage are concentrated in both necks inside an Active Damage Zone (ADZ) encompassing some volume of a severely transformed material with a specific damage morphology. The structural damage inside the ADZs reaches its critical level at the instant i (see Fig. 2) followed by the formation of two internal cracks within the necks. Subsequently they transform (at the state p) into two edge cracks (usually in turn) by the mechanism of internal necking. Taken together, these cracks represent a single Naturally Forming centre Crack (NFC) having the original length $2c_p$.

Further on, at the state $d0$ the NFC starts to propagate with an intermittent attainment of local instabilities, as shown in Fig. 2. Repeated cycles *loading-partial unloading-reloading* generate a cyclic variation in the crack geometry, which is bounded by the cracking and damaging curves shown in Fig. 3. The SST

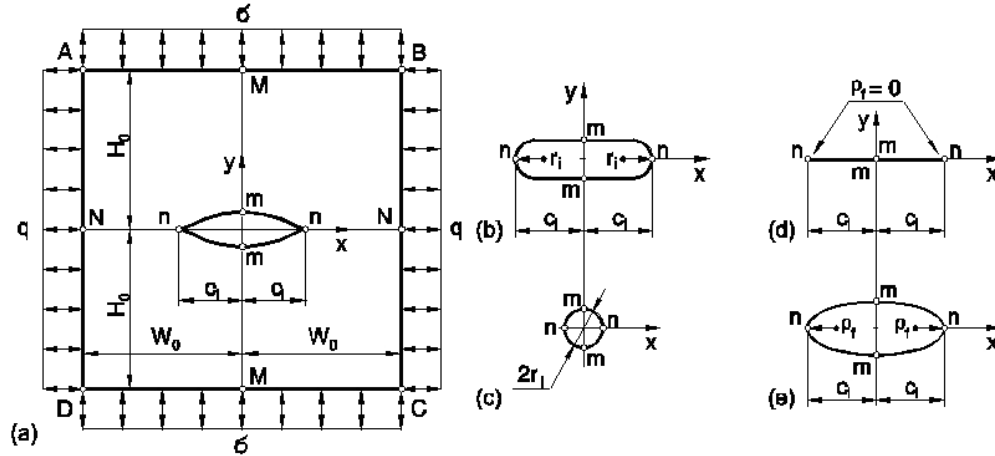


Fig. (1). The basic structural element ABCD with an original geometric imperfection of length $2c_i$ (a) and stress raisers with a well-defined geometry that are often used in fracture mechanics testing (b), (c) and analysis (d), (e).

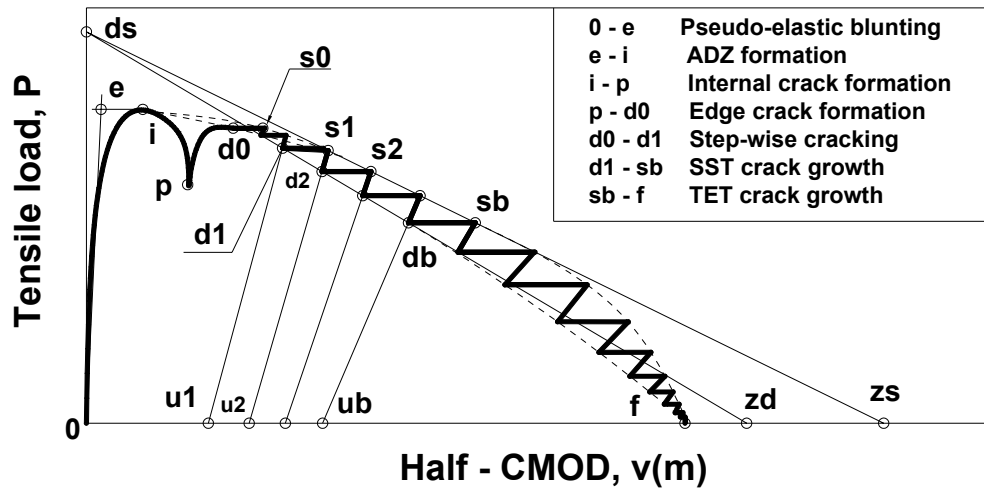


Fig. (2). Schematic diagram of ductile tearing initiated from a small geometric imperfection in a rectangular PD whose dimensions $2W_0$ and $2H_0$ are relatively large in comparison with its thickness B_0 . The imaginary cycles of *full unloading-reloading* (straight lines *du-ud*) are shown only for the SST range of crack extension.

regime of the crack extension is attained at the instant *d1* (Figs. 2 and 3) when the alternating process of cracking and damaging starts to occur in a self-similar manner. Thereafter the crack enters stage IV called Tail-End Tearing (TET), which comes to an end at the instant *f* of full separation.

The UM-based FFS procedure provides a three-level assessment of a through centre crack depending on the application and service requirements. Level 1

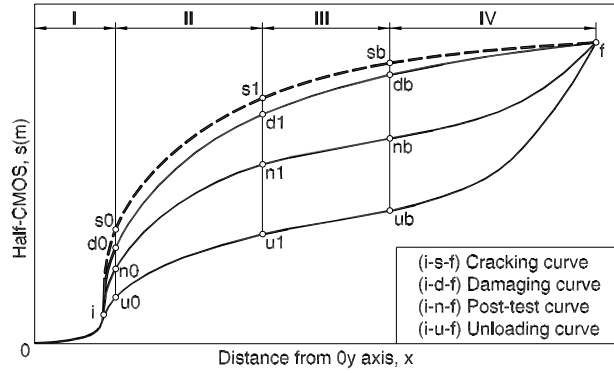


Fig. (3). Schematic presentation of continuous fracture curves related to each other by imaginary (instantaneous) *unloading–reloading* cycles performed at the moment “0” of the attainment of the critical damage at the tips of a through centre crack (states $d0-u0-s0$), moment “I” of the beginning of the SST crack growth stage ($d1-u1-s1$), and moment “b” of the transition to the TET ($db-ub-sb$).

assessment is performed by a simplified method that is quick and inexpensive, Level 2 assessment involves the use of a method of general application, and Level 3 assessment is based on an advanced procedure that provides greater accuracy of predictions. The choice of the method depends on the material and input data available, level of conservatism accepted, and degree of complexity required. In what follows they are referred to as L1, L2, and L3 methods.

3. L methods in outline

The L1 method aims at quantifying two instability events, namely, the initiation of cracking (state i in Figs. 2 and 3) and beginning of the SST crack growth stage (states $d1$ and $s1$). Both test events occur in a rectangular PD called MR(T) specimen. Its particular shape is displayed in Fig. 4b. The inner PD boundary has the form of an open hole with a specific radius $2r_0$. The width $2W_0$ of the MR(T) specimen whose horizontal boundaries are rigidly clamped is taken equal to that of the standard specimen (Fig. 4a). Because of a relatively small thickness-to-width ratio the characteristics of plastic flow and cracking are not affected by buckling, i.e., by out-of-plane displacements. To assess the effect of in-plane constraint on instability parameters of plastic flow and fracture, it is necessary to test specimens with different shape ratios $\lambda = H_0/W_0$, as it was done in [10].

The critical values of the tensile stress σ_{ni} and strain ε_{ni} in the vicinity of fracture nucleation sites (points n in Fig. 4b) should be obtained from elastic calculations based on Neuber’s analysis [11]. It makes use of the energy equivalence between the elastic and the elastic-plastic stress-strain fields, which has the form of an equality between the total values of the elastic strain energy density ($\sigma_n^e \times \varepsilon_n^e$) and the elastic-plastic strain energy density ($\sigma_n^{ep} \times \varepsilon_n^{ep}$). This way provides a quick

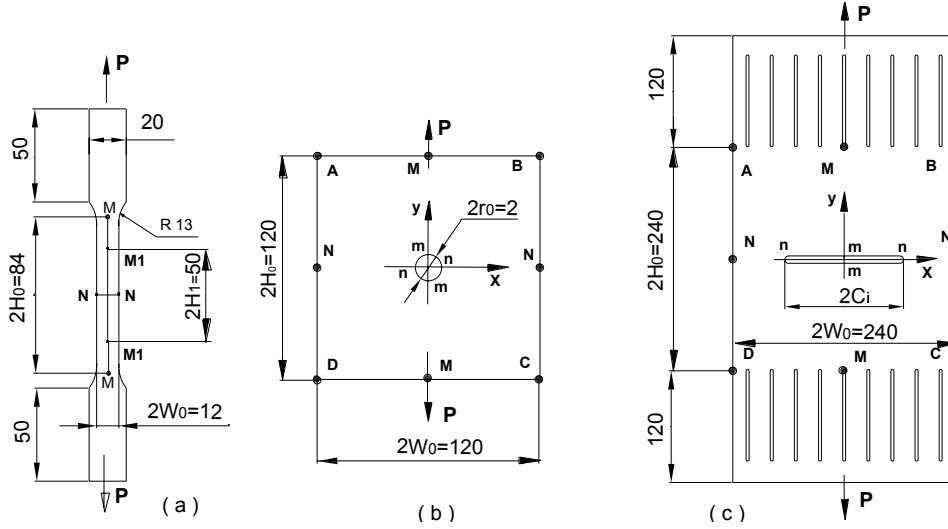


Fig. (4). The geometry of a standard tensile test specimen (a) shown together with the geometries of an MR(T) (b) and an MM(T) (c) specimen used in this study (all dimensions are in mm).

determination of the elastic-plastic stress σ_{ni}^{ep} and strain ε_{ni}^{ep} from the critical values of the elastic stress σ_{ni}^e and strain ε_{ni}^e . The second instability is characterised by the critical values of the net-section stress σ_{Nd} , specific work of fracture A_d , and the Crack Tip Opening Angle (CTOA- ψ) [2-8]. It is necessary to determine two CTOA- ψ parameters one of which (ψ_d) is related to the $ds-zd$ line in the test records (Fig. 2) and the other (ψ_n) to the $i-n-f$ curve (Fig. 3).

The L2 method also provides a point-by-point estimation of plastic flow and cracking jointly with a through-life assessment of tearing initiated from a hypothetical (point-wise) imperfection at the central point of an MR(T) or an M(T) specimen. They differ only in the shape of the original stress raiser shown in Figs. 1c and 1b, respectively. Here the in-plane dimensions $2W_0$ and $2H_0$ should be reasonably large (by 1-2 orders of magnitude larger than the PD thickness B_0). The MR(T) specimens with a circular hole and geometrically similar M(T) specimens with an elongated notch are tested without guide plates preventing the out-of-plane displacement. These specimens buckle only after a sufficiently large crack length-to-thickness ratio is attained. All measures of tearing resistance obtained for a shorter crack are not affected by buckling. Similarly to the L1 method, the effect of in-plane constraint is assessed from tests of specimens having widely different shape ratios λ .

Finally, the main objective of the L3 method is an in-depth analysis of the SST crack growth in a Basic Structural Element (BSE) (Fig. 1a). Its physical counterpart for the case of uniaxial tension is called MM(T) specimen (Fig. 4c). Its dimensions $2W_0$ and $2H_0$, as well as the corresponding dimensions of the MR(T) specimens used in the L2 method, should be relatively large in

comparison with the thickness B_0 . However, only elongated stress raisers of different lengths should be introduced into MM(T) specimens. Each specimen before testing should be lightly clamped (to minimize friction) by two guide plates for decoupling the fracture behaviour from the effects of buckling. The displacement-based parameters of the near crack-tip profile during the SST fracture and the procedure for their determination are partly presented in [8].

4. Material and experimental findings

The test material is aluminium alloy D16AT in as-received condition, having the form of 1.4-1.5mm thick sheets. Two sets of standard specimens (Fig. 4a) were loaded under quasi-fixed grip conditions (with the rate 0.001 mm/s) in tension across and along the rolling direction of the sheets. The elastic and anisotropic plastic behaviour under uniform deformation was characterized by the following parameters: the elastic modulus $E = 67.7$ GPa, Poisson's ratio $\nu = 0.32$, the 0.2% offset yield strength $\sigma_Y = 300$ and 338MPa, and the ultimate tensile strength $\sigma_{UTS} = 446$ and 467MPa, respectively. It should be emphasized that tearing always occurred by cracking in the plane inclined at 45° to the loading direction.

As can be seen from Fig. 5, the critical values of averaged tensile stresses for standard specimens with widely different λ ratios almost coincide. A similar lack of sensitivity to the λ variation was also observed in tests of the MR(T) specimens when the fracture nucleation occurred under non-uniform deformation. However, the softening branch of the test records for these specimens is noticeably affected by the variation of the in-plane constraint. Such effects were also observed in tests of the MR(T) specimens with the width $2W_0=120$ mm. A more detailed discussion of constraint effects is presented in [2-8,10]. The second experimental finding concerns the problem of collecting test data on the pop-in fracture behaviour of the MR(T) specimens of larger size. In Fig. 6 the local instabilities are visible as small dips on the softening branch of the diagram. They reflect a cyclic variation in the global crack geometry. For identical specimens, the increase in the loading rate up to (0.1 - 0.01) mm/s was always accompanied by a complete disappearance of the dips on all test records.

The next two findings are related to the problem of decoupling the effects of tearing from those of buckling. In the MR(T) specimens of size $2W_0 \times 2H_0 = 120 \times 120$ mm the out-of-plane displacements $w(m)$ were measured continuously near the points m (see Fig. 4b). The variation of its average values with the load reduction (Fig. 7) is induced by joint effects of the applied load P , crack aspect ratio c/W_0 , and crack length-to-thickness ratio c/B_0 on the compressive stress acting along the crack growth line. What is unexpected and hard to explain is the well-reproducible difference between the diagrams for identical specimens with cracks growing across and along the rolling direction.

Finally, an example of the through-life fracture curve expressed in terms of the residual CTOA- ψ_n values is displayed in Fig. 8. It was constructed from the data

on post-test crack profiles for completely fractured MM(T) specimens of the size $2W_0 \times 2H_0 = 240 \times 240 \text{mm}$. These specimens were tested with the use of guide plates preventing buckling. Tear cracks emanating from the tips of original notches of length $2c_i = 15, 30, 45,$ and 60mm were growing in a step-wise manner, as it was demonstrated in [8]. Predictive calculations of plane stress tearing can be made using the overall curve $\psi(x)_n$, as well as three characteristic angles shown in Fig. 8.

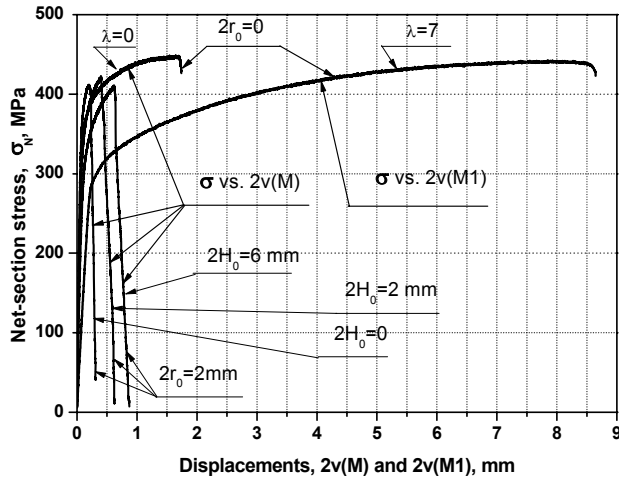


Fig. (5). Continuous test diagrams recorded under quasi-fixed grip conditions for the unconstrained ($\lambda \approx 7$) and highly constrained ($\lambda \approx 0$) specimens of width $2W_0 = 12 \text{mm}$ whose PDs contained no original stress raisers. They are shown together with similar diagrams for MR(T) specimens of the same width having different shape ratios λ (loading across the rolling direction).

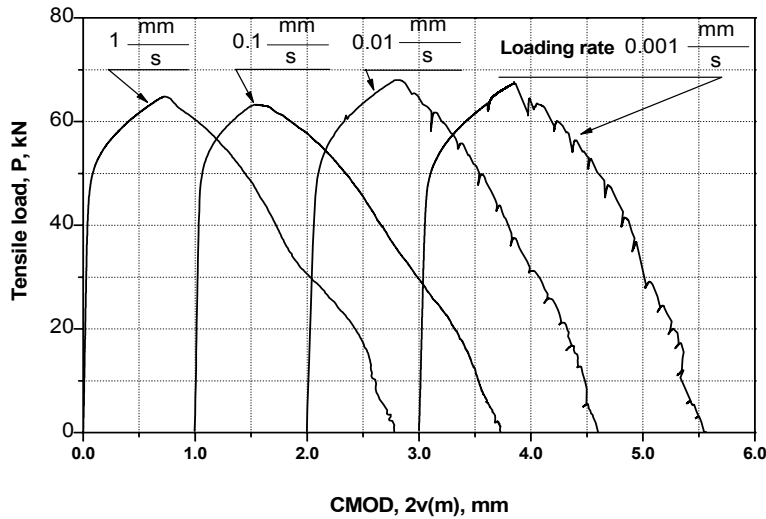


Fig. (6). Comparison of test records for four identical MR(T) specimens of size $120 \times 120 \text{mm}$ with an original hole of diameter $2r_0 = 2 \text{mm}$. The slanted cracks were growing along the rolling direction under displacement-controlled tension with the indicated loading rates.

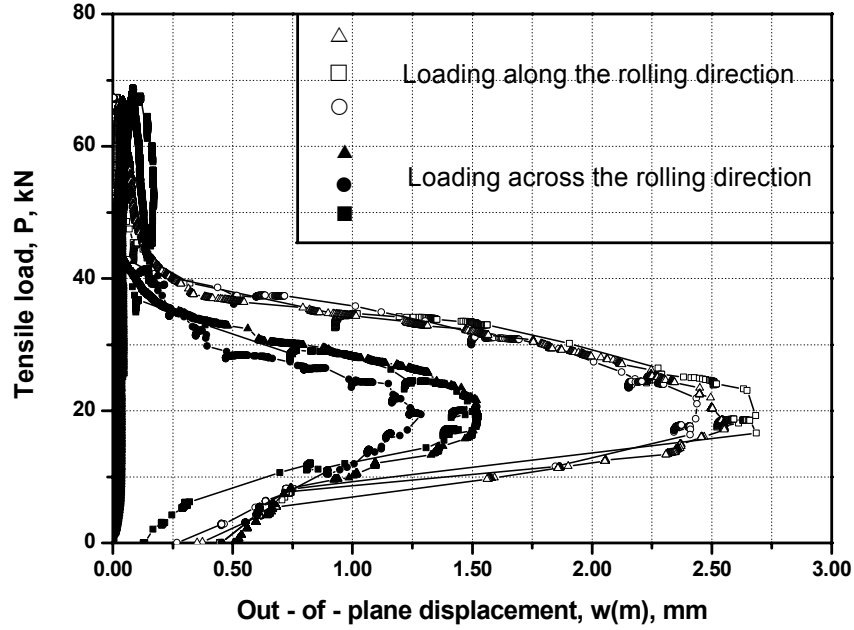


Fig. (7). Test records for two sets of identical MR(T) specimens of size $120 \times 120 \text{ mm}$ with an original hole of diameter $2r_0 = 2 \text{ mm}$ that were loaded with the rate 0.001 mm/s . The slanted cracks were growing along and across the rolling direction in the specimens of the first and second sets, respectively.

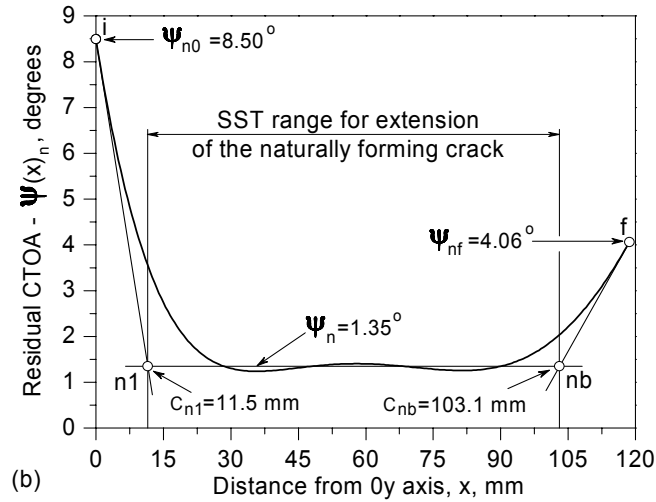


Fig. (8). CTOA-based characterization of an idealized tearing process initiated from a hypothetical imperfection of a negligibly small size in an MM(T) specimen with the PD dimensions $2W_0 \times 2H_0 = 240 \times 240 \text{ mm}$ (loading across the rolling direction).

5. General remarks

The CTOA-angles in Fig. 8 can be compared with the residual SST angles for the specimens of another shape and size partly presented in [2-8,10]. This comparison demonstrates that underlying assumptions of the currently used CTOA-based assessment of ductile tearing evoke a suspicion from different points of view. For example, the microtopography approach for the characterization of ductile fracture [12] assumes that the crack surfaces, in their final shape, contain the entire crack growth history. Consequently, the CTOA-based assessment of cracking can be performed using post-test measurements. These presumptions are included in the standard procedure [13] implicitly stating that the results of microtopography analysis must be similar to those obtained by direct measurements on a loaded specimen with the use of an optical microscope. This assumption contradicts the above experimental results [2-8,10].

The available data on validation of the three-level procedure in question allow making, at least, the following conclusion. The L1 method is an attractive alternative to the test procedure for determining the essential work of fracture. The latter is now the most popular express method for assessing the fracture behaviour of thin-sheet materials. Unlike this procedure, the L1 method gives quick, inexpensive, and yet accurate estimations of the critical stress σ_{ni} and strain ε_{ni} for fracture nucleation sites in the vicinity of a typical stress raiser. Additionally, the L1 method provides stress-, displacement-, and energy-based measures of a material's resistance to the onset of SST crack growth.

When determined by the L1 and L2 methods, the above instability parameters have the advantage of being directly related to particular positions of stationary and advancing crack tips. Besides, the critical stresses σ_{ni} and σ_{Nd} , as well as the strain ε_{ni} , are closely related to such customarily used quantities as the yield strength σ_Y and the ultimate tensile strength σ_u , and strain ε_u obtained under uniform deformation of a standard specimen. The overall result of this work indicates the importance of the specimen size and shape effects in the joint assessment of plastic flow, localized damaging, and cracking for tension-dominant crack geometries.

Acknowledgements

I am grateful to Mr. I.V. Limansky for kindly placing at my disposal the test records presented in Figs. 6 and 7.

References

- [1] FITNET, European Fitness-For-Service Network, Final report for Work Package 2 State-of-the-Art and Strategy, October 2003.
- [2] V.P. Naumenko and G.S. Volkov, Assessment of plane stress tearing in terms of various crack-driving parameters, in: *Fatigue and Fracture Mechanics*, ASTM STP1461, S. R. Daniewicz, J. C. Newman, Jr., and K.-H. Schwalbe, Eds. West Conshohocken, PA: ASTM International, (34), (2003), pp. 182-202.
- [3] V. P. Naumenko, Yu. D. Skrypnyk and N. I. Nedelchev, Constraint-dependent fracture toughness of glass and PMMA,” in *Proc. of the ICF11 International Conference on Fracture*, A. Carpintery, Ed., Turin, Italy, (2005).
- [4] V.P. Naumenko, Incorporation of Length Scale in Plane Stress Fracture Analysis, in *Proc. of the ECF16, Fracture of Nano and Engineering Materials and Structures*, E.E. Gdoutos, Ed., Alexandropoulos, Greece, (2006).
- [5] V. P. Naumenko and Yu. D. Skrypnyk, “Sensitivity of crack nucleation parameters to the geometric imperfection”, in *Proc. of the ECF16 Fracture of Nano and Engineering Materials and Structures*, E. E. Gdoutos, Ed., Alexandropoulos, Greece, (2006).
- [6] V.P. Naumenko, A.G. Atkins, Engineering Assessment of Ductile Tearing in Uniaxial and Biaxial Tension, *International Journal of Fatigue*, (28), No. 5-6, (2006), pp. 494-503.
- [7] V.P. Naumenko, S.V. Lenzion, E.V. Vasylyev, Yu.D. Skrypnyk, Yu.L. Shyrynkin, Constraint-Dependent Characteristics of Plane Stress Tearing Resistance, in *Proc. of the ICMFF8*, Sheffield, UK, (2007).
- [8] V.P. Naumenko, S.V. Lenzion, and I.V. Limansky, Displacement-Based Assessment of Ductile Tearing under Low-Constraint Conditions, *The Open Mechanical Engineering Journal*, (2), (2008), pp.40-59.
- [9] V.P. Naumenko, G.S. Volkov, and A.G. Atkins, Initiation and propagation of ductile tearing: A search for biaxial fracture criterion, in the *Sixth International Conference on Biaxial/Multiaxial Fatigue and Fracture*, M. M. de Freitas, Ed. Lisboa, 2001, pp. 975-982.
- [10] V.P. Naumenko, S.V. Lenzion, and Yu. D. Skrypnyk, Ductile Tearing in Narrow and Wide Strips of Thin-Sheet Aluminium Alloy, in the *Proceedings of the ESIA8, Through-life Management of Structures and Components*, Manchester, UK, 2006, 10 pages.
- [11] H. Neuber, Theory of stress concentration for shear strained prismatic bodies with arbitrary nonlinear stress-strain law, *ASME J. Appl. Mech.*, (29), (1961), pp. 544-550.
- [12] W. R. Lloyd, Microtopography for ductile fracture process characterization. Part 1: Theory and methodology, *Eng. Fract. Mech.*, (70), (2003), pp. 387-401.
- [13] Working document ISO/TC 164/SC 4 N413.3, *Metallic Materials Method of Test for the Determination of Resistance to Stable Crack Extension Using Specimens of Low Constraint*, (2004).